

## Study the Effect of Coating by TiO<sub>2</sub> Nano-Particles on Carbon Steel Behavior via. Sol-Gel Method

<sup>1</sup>Mustafa J. Azeez, <sup>2</sup>Ali H. Ataiwi, <sup>1</sup>Ali A. Abdulhadi and <sup>3</sup>Mohammed H. Shinen

<sup>1</sup>Department of Materials, College of Engineering, University of Kufa, Kufa, Iraq

<sup>2</sup>Department of Materials Engineering, University of Technology, Baghdad, Iraq

<sup>3</sup>Department of Science, College of Basic Education, University of Babylon, Hillah, Iraq

---

**Abstract:** The use of nanoparticles has become very important in many industrial applications for its important role in improving all the properties including thermal, electrical, mechanical and chemical in the different environments. In this study, TiO<sub>2</sub> nanoparticles used to improve corrosion resistance of carbon steel by using a sol-gel method. Coating of nanoparticles done by using a spin coating method. Several tests such as XRD, SEM and EDS were used to analyze the morphology, crystalline phase and composition of coatings. The corrosion resistance of nanoparticles evaluated using Tafel polarization and electrochemical impedance analysis. The results showed a homogeneous distribution of nanoparticles on the surface of carbon steel without cracks and flaking off from substrate. Also, corrosion resistance for carbon steel was increased and  $i_{corr}$  was decreased from 27.72-0.4862  $\mu\text{A}/\text{cm}^2$ .

**Key words:** Spin coating, TiO<sub>2</sub> nanoparticle, mild steel, corrosion behavior, carbon,  $i_{corr}$

---

### INTRODUCTION

Corrosion can make terrible harmful to metal and alloy structures causing monetary results as far as repair, substitution, product and safety losses and ecological contamination (El-Lateef and Tantawy, 2016). Mild steel has a standout utilized amongst the most essential and broadly materials there are different strategies to secure protective steel against consumption in harsh situations (El-Lateef, 2015). Organic coatings are nearly always a barrier coating that is to say they provide corrosion protection by forming a barrier between the substrate and the atmosphere and if this is broken protection ceases (Fedrizzi *et al.*, 2008). Ceramic coatings are like wise exceptionally appealing as covering materials, since, they have great thermal and electrical properties and they are more impervious to wear, corrosion and oxidation than metals in forceful conditions having high temperature (Wachtman and Haber, 1993). Ceramics oxide barriers and coatings like titania, silica, zirconia and alumina can be kept on metals to enhance their surface properties (Cheraghi *et al.*, 2012; Curkovic *et al.*, 2013). Sundry techniques used to acquire ceramics coatings on metallic surfaces like, plasma spraying, physical vapordeposition, chemical vapordeposition, laser cladding and chemical plating or sol-gel technique. The sol-gel process has featured characteristics over the other processes due to premium compositional control, homogeneity on the

molecular level due to the mixing of liquid precursors and lower crystallization temperature. This process is environmentally friendly, less expensive, gave us materials of good purity and excellent homogeneity of the microstructure, also can be controlled on pore size, pore volume and surface area of deposited film (Brinker and Schere, 1990). In order to improve the corrosion resistance we have to apply the protective or coating layers homogenously and without cracks. The existence of defects and cracks in the coating layers will lead to localized corrosion (Gluszek *et al.*, 1990). Recently, the corrosion behavior of different samples of aluminum alloys, carbon steel and stainless steels has been studied using sol-gel coatings (Khalaf and El-Lateef, 2016). Spin coating is one of the most common sol-gel techniques for thin film deposition; this consists in the deposition a small amount of coating material on the center of the substrate which is spinning at specific speed and then rotated at high speed to disperse the coating material by centrifugal force. Because of the numerous uses of carbon steel in industry applications, this researche demonstrates an endeavor to increase the corrosion resistance properties of mild steel substrate by applying TiO<sub>2</sub> nanoparticle coating utilizing the sol-gel technique. The phase composition, morphology and the elemental distribution of TiO<sub>2</sub> thin films have been analyzed by X-Ray Diffraction (XRD), Scanning Electron Microscopy (SEM) and Energy Dispersive X-ray Spectroscopy (EDS).

Tafel extrapolation and impedance analysis were utilized to evaluate the corrosion resistance of the TiO<sub>2</sub> coatings in 3.5% NaCl solution and discuss the obtained results.

**MATERIALS AND METHODS**

**Experimental:** Titanium Dioxide (TiO<sub>2</sub>) had been prepared by of Sol-Gel method with the use of Titanium Isopropoxide (TIP) (C<sub>12</sub>H<sub>28</sub>O<sub>4</sub>Ti) with purity of (98%), acetic Acid (CH<sub>3</sub>COOH) with purity of (99.5%) and ethanol (C<sub>2</sub>H<sub>5</sub>OH) with purity of (99.7%). These materials were produced by Aldrich Chemicals Company.

**Preparation of carbon steel substrate:** The surface of mild steel substrate is an important factor in the calculation of corrosion resistance, so, it is necessary to prepare a regular surface. Specimens of mild steel in form of (20×15×3 mm) were ground with silicon carbide papers in sequence of No. 220-2000 grit to get flat and scratch-free surface by grinder and polisher and then ultrasonically cleaned in ethanol and distilled water, respectively .The specimens are air-dried and the deposition process followed. Carbon steel (St 52-3 DIN 17100) was used in this research, the chemical composition of mild steel is shown in Table 1.

**Preparation TiO<sub>2</sub> solution by sol-gel method:** TiO<sub>2</sub> solutions are prepared by Sol-Gel spin-coating method. About 25 mL of ethanol was mixed for 30 min then 2.5 mL of acetic acid was added to ethanol and stirred by using a magnetic stirrer for 4-7 min and measure of 3.2 mL of TIP was added by pipette to a beaker containing the mixture of glacial acetic acid and ethanol that had been mixed for 4 min. The mixture was continually stirred using a magnetic stirrer and for a further 2 min after addition of the precursor.

**Preparation of TiO<sub>2</sub> thin films:** Specimens were spin coated by the TiO<sub>2</sub> solution with a spinning speed between 500 and 2500 rpm for one layer of coating and 1500 rpm for several coating layers. The second layer was coated after completing the process of annealing for the first layer. The time of rotating speed was 40 sec for each specimen. After coating, specimens were annealed at 550°C with heating rate of 3°C/min as shown in Fig. 1. The flow chart of preparation of TiO<sub>2</sub> thin films given in Fig. 2

**Coating thickness measurement:** At different conditions of coatings, the thickness of coatings has been measured

by gravimetric method. This method conducted by measuring the weight of the coated layer then calculating the thickness from the densities of the material and the geometric surface area. The thickness was calculated as follow (Eq. 1):

$$T = \frac{w}{A \times s} \tag{1}$$

Where:

T = The Thickness

w = The weight

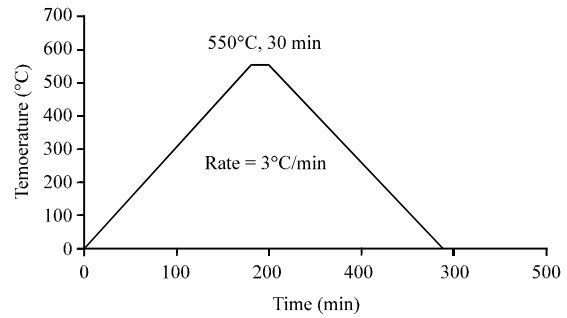


Fig. 1: Heat treatment after coating process

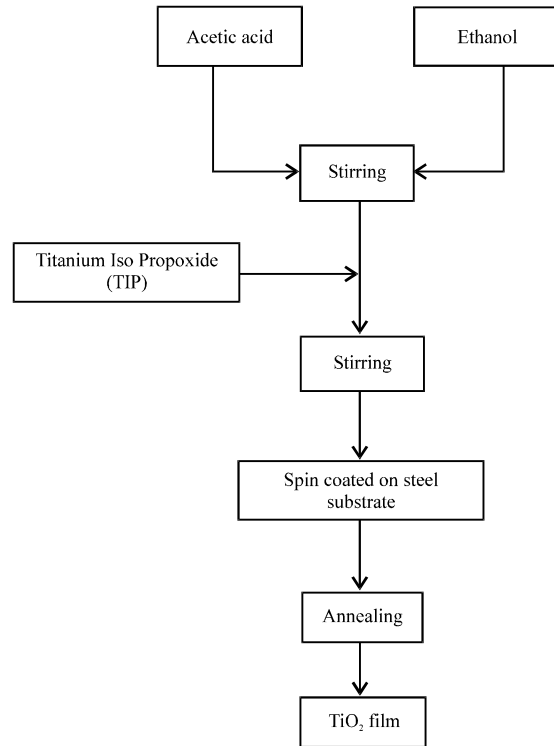


Fig. 2: Flow chart of preparation of TiO<sub>2</sub> thin films

Table 1: Chemical composition of carbon steel

Metal	C	Si	Mn	S	P	Cr	Ni	Al	Cu	Mo	V	Fe
Wt.%	0.112	0.264	0.687	0.010	0.010	0.020	0.028	0.049	0.022	0.002	0.003	Bal

A = The surface Area  
 d = The density

**Corrosion measurements:** Tafel extrapolation strategy was utilized to evaluate corrosion current density and corrosion potential values. A three electrode cell with the coated substrates as a working electrode, saturated calomel electrode as a reference electrode and a platinum plate as a counter electrode was utilized as a part of the tests. The test area of working electrode was 1 cm<sup>2</sup>. The primary modified advance in this estimation is open circuit potential and the polarization bend will begin at open circuit potential over a potential range about ±200 mV from the open circuit. The electrochemical measurement test was performed at room temperature (32°C) in 3.5 wt. % NaCl solution. After the electrochemical testing system ended up stable (around 60 min), scans were conducted at a rate of 1 mV/sec. Open circuit potential (E<sub>corr</sub>) was estimated in the wake of achieving a steady state and afterward the polarization estimations were finished. The polarization resistance was evaluated by the relationship (Clement *et al.*, 2012):

$$R_p = \left[ \frac{b_a b_c}{2.303(b_a + b_c) i_{corr}} \right] \quad (2)$$

Where:

i<sub>corr</sub> = The corrosion current density  
 b<sub>a</sub> = Anodic Tafel slope  
 b<sub>c</sub> = Cathodic Tafel slope

The corrosion rate was calculated by Eq. 3 (Sekunowo *et al.*, 2013):

$$C_R (mpy) = 0.13 \times i_{corr} \times \left( \frac{e}{\rho} \right) \quad (3)$$

Where:

C<sub>R</sub> = The corrosion rate in mil per year  
 e = Equivalent weight  
 ρ = Density of carbon steel

The Protection Efficiency (PE %) also was estimated by the following Eq. 4 (Behpour *et al.*, 2008):

$$PE \% = \left[ 1 - \frac{i_{corr, coated}}{i_{corr, uncoated}} \right] \times 100 \quad (4)$$

where, i<sub>corr,uncoated</sub> and i<sub>corr,coated</sub> are corrosion current densities for uncoated and coated substrates, respectively. The Porosity Percentage (PP %) was also evaluated as follows Eq. 5 (Lorenzetti *et al.*, 2014):

$$PP \% = \left[ \frac{R_{p, uncoated}}{R_{p, coated}} 10^{\frac{-\Delta E_{corr}}{b_a}} \right] \times 100 \quad (5)$$

Where:

R<sub>p,uncoated</sub> = The polarization resistances of the uncoated and R<sub>p,coated</sub> and coated substrates, respectively  
 • E<sub>corr</sub> = The corrosion potential difference between them  
 b<sub>e</sub> = The anodic Tafel slop of the uncoated substrate

**Characterization of coated surfaces:** X-ray diffraction analysis was used to characterize the element and phases on the uncoated and coated surfaces. The surface morphology and elemental distribution of coated surfaces were investigated by scanning electron microscope equipped with a sing Energy Dispersive Spectroscopy (EDS), respectively.

## RESULTS AND DISCUSSION

XRD analysis was used to characterize the element and phases on the uncoated and coated surfaces. Figure 3 shows the XRD spectrum of uncoated surface which indicates the presence of iron as a main element in steel. The XRD of uncoated steel is agreed with the Card No. (03-1050) according to JCPDS program. The other details are listed in Table 2.

Figure 4 shows the XRD analysis of TiO<sub>2</sub>-coated carbon steel. This figure indicates the presence of titanium dioxide as anatase and rutile that agreed with the Card No. (01-1197) according to JCPDS program in addition to the appearance of the peaks for iron and iron oxides (Fe<sub>2</sub>O<sub>3</sub>, Fe<sub>3</sub>O<sub>4</sub> and FeOOH). The other details are listed in Table 3.

The surface morphology and particle distribution of titanium dioxide in carbon steel was performed by using SEM. Figure 5 shows clearly the shape of the clustering and particles of TiO<sub>2</sub> on metal surface.

Figure 6 shows the mapping data of EDS spectrum for analyzed surface of carbon steel specimens that coated with TiO<sub>2</sub>. These images present elements distribution of (TiO and Fe) in the coated surface.

The results in Table 4 indicates that the increasing in speed of spinning leads to decreasing in thickness due to loss more amount of coating emulsion with getting more compacted layer. At the same speed, we can see that the increasing of deposit layer led to increasing in thickness because of deposit more material on metallic surface.

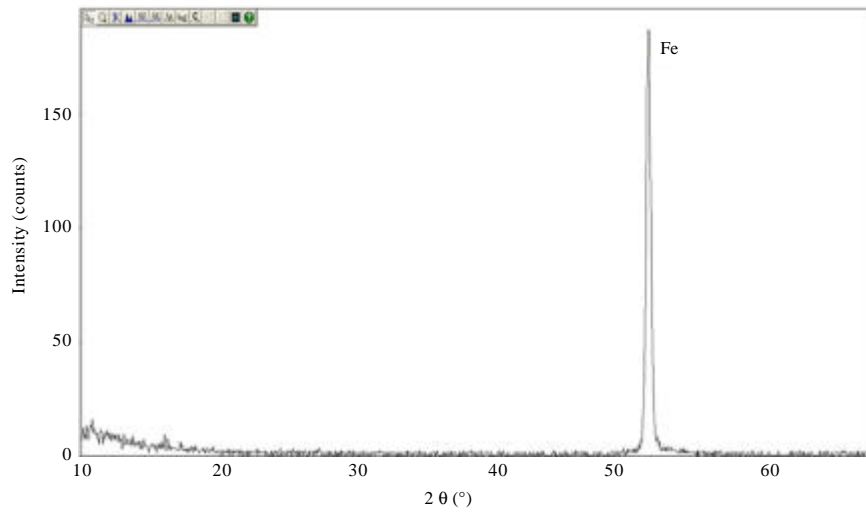


Fig. 3: The X-ray diffraction pattern of uncoated carbon steel

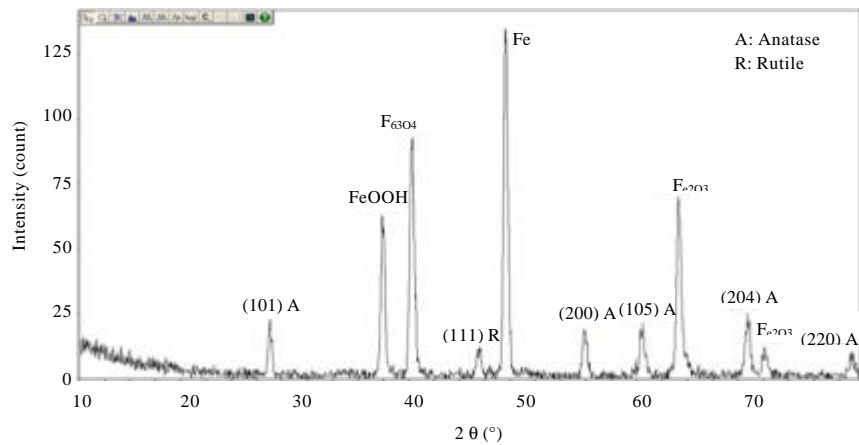


Fig. 4: The X-ray diffraction pattern of coated carbon steel

Table 2: The X-ray diffraction pattern of uncoated carbon steel

Variables	2•	d-spacing (nm)	Rel. Int. (%)	FWHM
1	45.920	0.19746	100.0	0.314

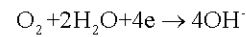
Table 3: The X-ray diffraction pattern of coated carbon steel

Variables	2•	d-spacing [nm]	Rel. Int. [%]	FWHM
1	25.074	0.35486	12.6	0.306
2	33.902	0.26420	46.7	0.326
3	36.299	0.24728	68.9	0.376
4	41.658	0.21663	8.9	0.286
5	43.640	0.20724	100.0	0.346
6	49.940	0.18247	13.3	0.395
7	54.520	0.16817	15.6	0.411
8	57.339	0.16056	50.4	0.417
9	62.882	0.14767	16.3	0.399
10	64.142	0.14507	8.9	0.267
11	70.996	0.13265	7.4	0.354

Table 4: Thickness of the coated layers

Speed of coating (rpm)	Thickness (µm)
500	3.2734
1000	2.2041
1500	1.0748
2000	0.6217
2500	0.2771
1500 (2 layers)	2.2536
1500 (3 layers)	3.4721

This figure indicates the cathodic region where the reduction of oxygen can occur as follows:



While at anodic region, the dissolution of iron takes place to form ferrous ions according to the following reaction:

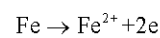


Figure 7 shows the polarization curve of uncoated carbon steel in 3.5% NaCl solution at room temperature.

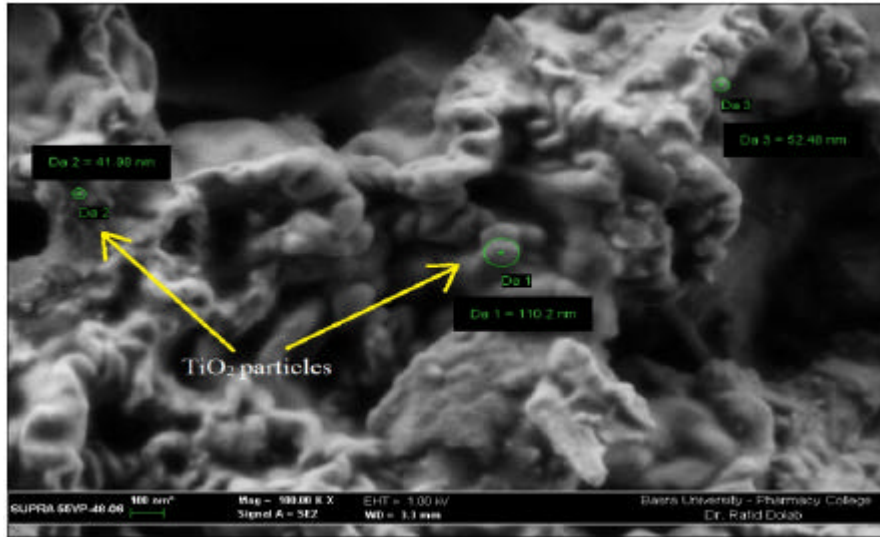


Fig. 5: SEM images showed nano particles of  $\text{TiO}_2$  on carbon steel

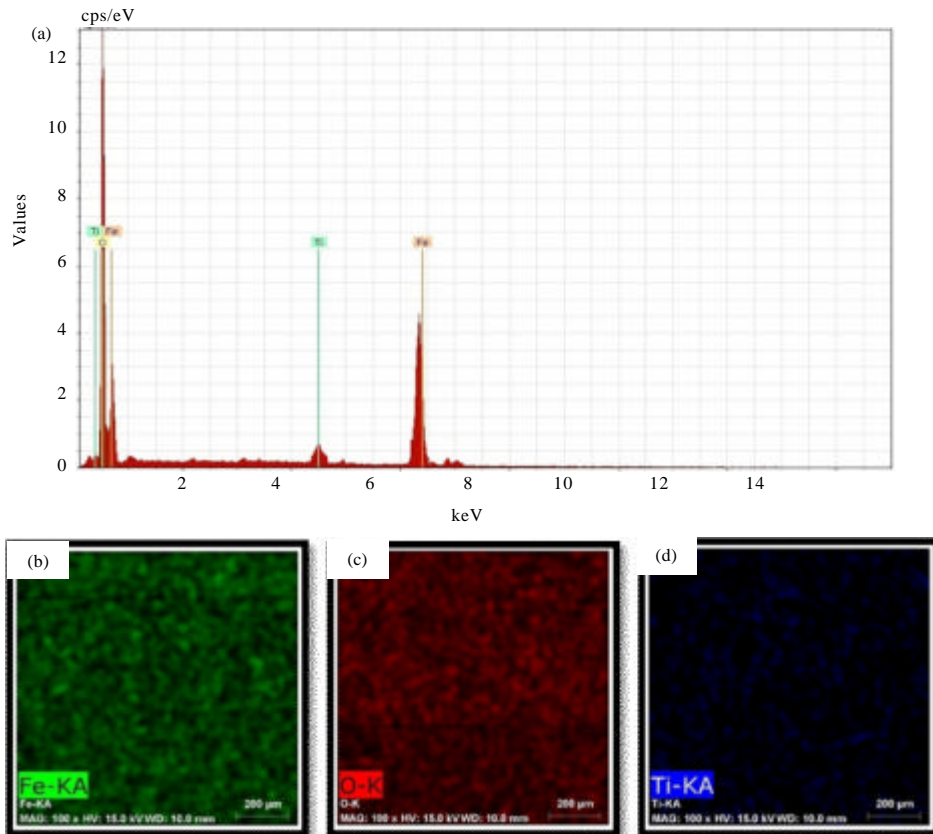


Fig. 6: a-d) EDS mapping of carbon steel coated with  $\text{TiO}_2$

Corrosion parameters were calculated by Tafel extrapolation method. These parameters include corrosion potential ( $E_{\text{corr}}$ ), corrosion current density ( $i_{\text{corr}}$ ) and Tafel

slopes ( $b_c$  and  $b_a$ ). The corrosion potential of uncoated specimen is  $-276.9$  mV and the corrosion current density is  $27.72 \mu\text{A}\cdot\text{cm}^{-2}$ .

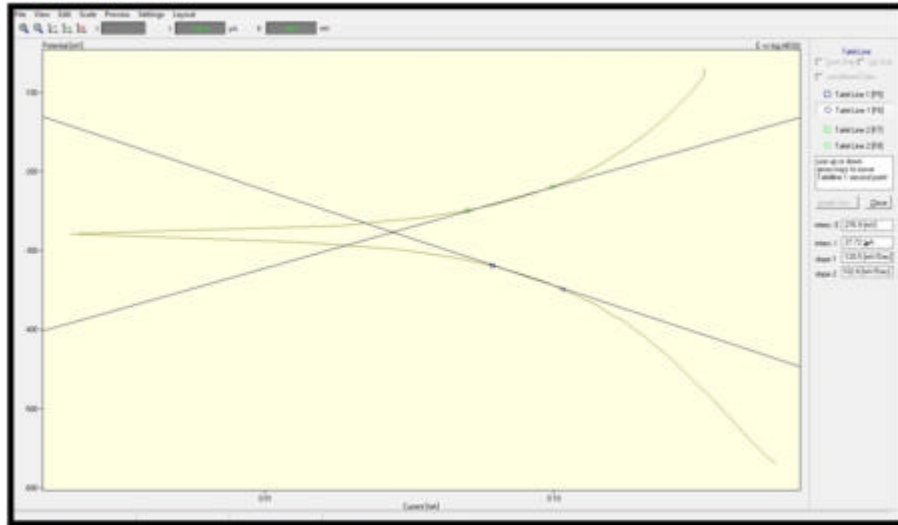


Fig. 7: Tafel plot of uncoated carbon steel in 3.5% NaCl solution at room temperature

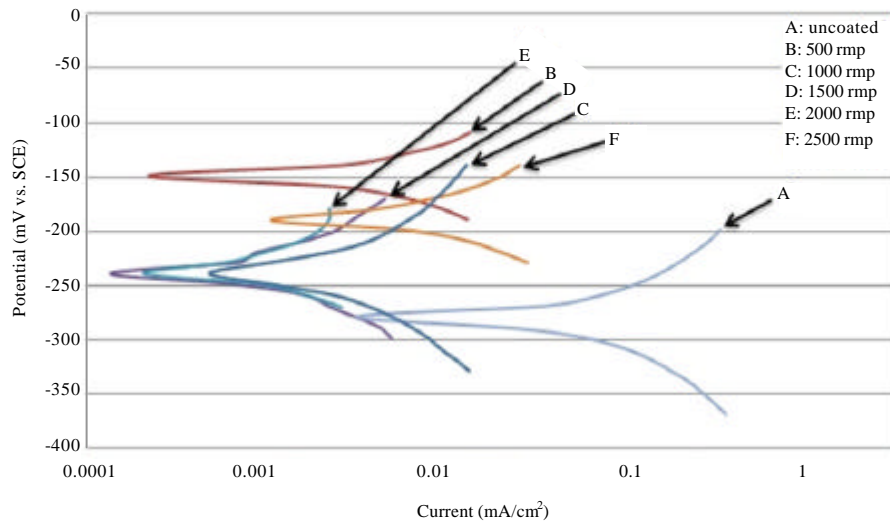


Fig. 8: Tafel plot curves for uncoated and coated specimens with one layer of coatings in 3.5% NaCl solution

Table 5: Measured corrosion data of uncoated and coated specimens with one layer of coatings in 3.5% NaCl solution

Specimens	$-E_{cor}$ (mV)	$i_{cor}$ ( $\mu A.cm^{-2}$ )	$-b_a$ (mV.dec <sup>-1</sup> )	$+b_c$ (mV.dec <sup>-1</sup> )
Uncoated	276.9	27.72	120.5	102.8
Coated with 500 rpm	148.5	3.530	120.3	121.1
Coated with 1000 rpm	234.6	1.430	124.0	106.1
Coated with 1500 rpm	238.7	0.817	101.0	124.2
Coated with 2000 rpm	238.2	0.990	116.2	264.2
Coated with 2500 rpm	185.6	5.590	108.8	121.2

Figure 8 indicates the polarization curves of coated carbon steel with one layer of TiO<sub>2</sub> nano particle coatings and the data are listed in Table 5. These data indicate that the corrosion potential became more positive due to the presence of protective layer of TiO<sub>2</sub> in addition to the

formation of passive layer on steel surface. The corrosion current density was decreased for coated specimens due to reduce the dissolution of metal and then reducing the electrons production which results in reduction of corrosion.

Generally, the cathodic Tafel slope was decreased due to reduction of the cathodic reaction while the anodic Tafel slope was increased after coating because of the rapid transfer from active to passive regions.

The results listed in Table 6 and represented in Fig. 9 which indicated that one layer coating at speed of spinning of 1500 rpm has the highest Protection Efficiency (PE %).

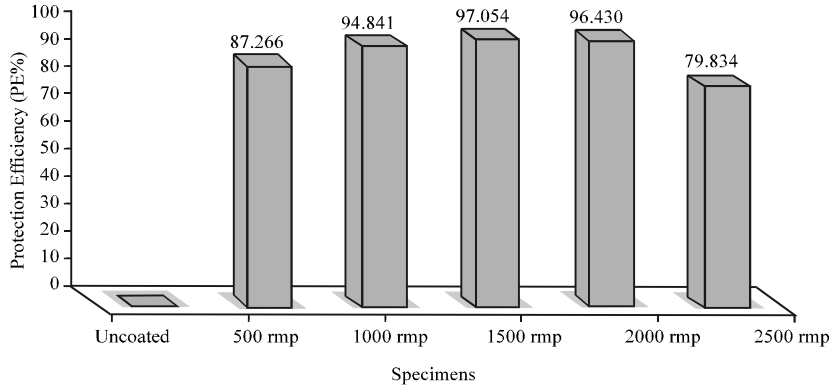


Fig. 9: Protection efficiency values for uncoated and coated specimens with one layer of coatings in 3.5% NaCl solution

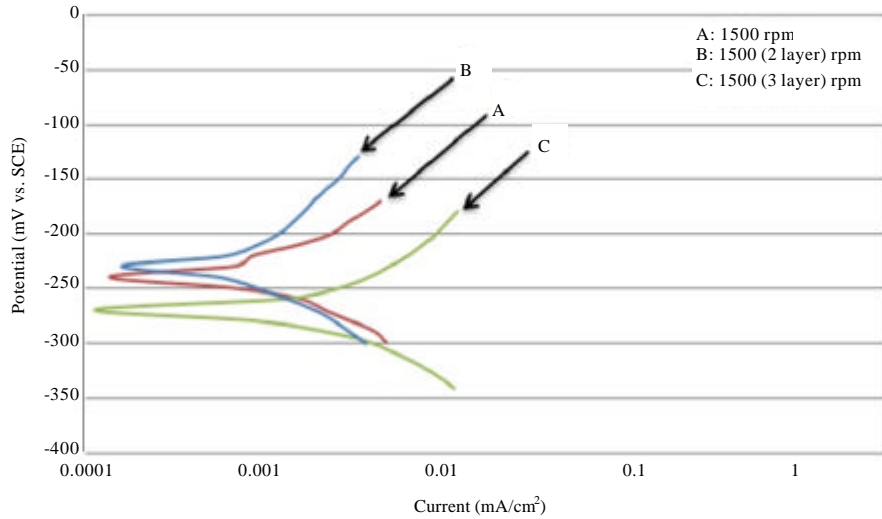


Fig. 10: Tafel plot curves for coated specimens with several layers of coatings in seawater

Table 6: Calculated corrosion parameters for coated specimens with one layer of coatings

Specimens	$R_p \times 10^3 (\cdot \text{cm}^2)$	$C_r$ (mpv)	PE (%)	PP (%)
Uncoated	0.86897	12.6882	-	-
Coated with 500 rpm	7.42342	1.6158	87.266	0.65974
Coated with 1000 rpm	17.36163	0.6545	94.841	1.94059
Coated with 1500 rpm	29.62269	0.3737	97.054	1.24676
Coated with 2000 rpm	35.41512	0.4529	96.430	1.03123
Coated with 2500 rpm	4.45346	2.5587	79.834	2.52449

Table 7: Measured corrosion data of coated specimens with layers of coatings in seawater at 1500 rpm

Specimens	$-E_{corr}$ (mV)	$i_{corr}$ ( $\mu\text{A} \cdot \text{cm}^{-2}$ )	-bc (mV.dec <sup>-1</sup> )	+ba (mV.dec <sup>-1</sup> )
Coated with 1 layer	238.7	0.8165	101.0	124.2
Coated with 2 layers	220.3	0.4862	110.1	120.8
Coated with 3 layers	268.0	1.5200	108.8	118.5

Table 8: Calculated corrosion parameters for coated specimens with several layers of coatings

Specimens	$R_p \times 10^3 (\cdot \text{cm}^2)$	CR (mpv)	PE (%)	PP (%)
Coated 1 layer	29.62269	0.3737	97.054	1.24676
Coated with 2 layers	51.44559	0.2225	98.246	0.47542
Coated with 3 layers	16.20355	0.6957	94.517	4.39358

The data in Table 6 indicate that the coated specimens have more corrosion resistance than that of uncoated ones. On the other hand, the results show that increasing speed of spinning lead to increasing the porosity because of losing more amount of coating emulsion.

Figure 10 shows the polarization curves of coated carbon steel with two and three layers of coatings. The data of corrosion refers that the coating with two layers has the nobler corrosion potential, lowest corrosion rate (current density), highest efficiency and resistance and lowest porosity when it is compared with coating of one and 3 layers as listed in Table 7 and 8.

### CONCLUSION

Properties of TiO<sub>2</sub> nanoparticle coating are high homogeneity of surface, no crack and good adherence,

these properties increase the corrosion resistance. Layer of TiO<sub>2</sub> coating assists to form passive layer on steel surface. To achieving high quality coating some parameters have been controlled such as concentration of solution, temperature of heat treatment, spinning speed and number of coating layers. Anatase phase determined by heating the surface of substrate at 550°C. Increasing speed of spin coating leads to increasing the porosity. The coating with two layers has the distinguished corrosion potential, lowest corrosion rate (current density), highest efficiency and resistance and lowest porosity compared with coating of 1 and 3 layers. Corrosion resistance of coated substrate was improved about 68 times than that of uncoated substrate.

### REFERENCES

- Behpour, M., S.M. Ghoreishi, N. Soltani, M. Salavati-Niasari, M. Hamadani and A. Gandomi, 2008. Electrochemical and theoretical investigation on the corrosion inhibition of mild steel by thiosalicylaldehyde derivatives in hydrochloric acid solution. *Corros. Sci.*, 50: 2172-2181.
- Brinker, C.J. and G.W. Scherer, 1990. *Sol-Gel Science: The Physics and Chemistry of Sol-Gel Processing*. 1st Edn., Academic Press, San Diego, ISBN-13: 978-0121349707, pp: 912.
- Cheraghi, H., M. Shahmiri and Z. Sadeghian, 2012. Corrosion behavior of TiO<sub>2</sub>-NiO nanocomposite thin films on AISI 316L stainless steel prepared by sol-gel method. *Thin Solid Films*, 522: 289-296.
- Clement, A., S. Laurens, G. Arliguie and F. Deby, 2012. Numerical study of the linear polarisation resistance technique applied to reinforced concrete for corrosion assessment. *Eur. J. Environ. Civ. Eng.*, 16: 491-504.
- Curkovic, L., H.O. Curkovic, S. Salopek, M.M. Renjo and S. Segota, 2013. Enhancement of corrosion protection of AISI 304 stainless steel by nanostructured sol-gel TiO<sub>2</sub> films. *Corros. Sci.*, 77: 176-184.
- El-Lateef, H.M.A. and A.H. Tantawy, 2016. Synthesis and evaluation of novel series of Schiff base cationic surfactants as corrosion inhibitors for carbon steel in acidic/chloride media: Experimental and theoretical investigations. *RSC. Adv.*, 6: 8681-8700.
- El-Lateef, H.M.A., 2015. Experimental and computational investigation on the corrosion inhibition characteristics of mild steel by some novel synthesized imines in hydrochloric acid solutions. *Corros. Sci.*, 92: 104-117.
- Fedrizzi, L., F. Andreatta, L. Paussa, F. Deflorian and S. Maschio, 2008. Heat exchangers corrosion protection by using organic coatings. *Prog. Org. Coat.*, 63: 299-306.
- Gluszek, J., J. Jedrkowiak, J. Markowski and J. Masalski, 1990. Galvanic couples of 316L steel with Ti and ion plated Ti and TiN coatings in Ringers solutions. *Biomater.*, 11: 330-335.
- Khalaf, M.M. and H.M.A. El-Lateef, 2016. Corrosion protection of mild steel by coating with TiO<sub>2</sub> thin films co-doped with NiO and ZrO<sub>2</sub> in acidic chloride environments. *Mater. Chem. Phys.*, 177: 250-265.
- Lorenzetti, M., E. Pellicer, J. Sort, M.D. Baro and J. Kovac *et al.*, 2014. Improvement to the corrosion resistance of Ti-based implants using hydrothermally synthesized nanostructured anatase coatings. *Mater.*, 7: 180-194.
- Sekunowo, O.I., S.O. Adeosun and G.I. Lawal, 2013. Potentiostatic polarisation responses of mild steel in seawater and acid environments. *Intl. J. Sci. Technol. Res.*, 2: 139-145.
- Wachtman, J.B. and R.A. Haber, 1993. *Ceramic Films and Coatings*. Noyes Publications, New York, USA., ISBN:9780815513186, Pages: 447.